Journal of Virology®

PATHOGENESIS AND IMMUNITY

LAP$^+$ Cells Modulate Protection Induced by Oral Vaccination with Rhesus Rotavirus in a Neonatal Mouse Model

Laura María Rey,[a] José Ángel Gil,[a,d] José Mateus,[b] Luz-Stella Rodríguez,[a] Martín Alonso Rondón,[c] Juana Ángel,[a] Manuel Antonio Franco[a]

[a]Instituto de Genética Humana, Facultad de Medicina, Pontificia Universidad Javeriana, Bogotá, Colombia
[b]Department of Microbiology, Pontificia Universidad Javeriana, Bogotá, Colombia
[c]Department of Clinical Epidemiology and Biostatistics, Pontificia Universidad Javeriana, Bogotá, Colombia
[d]Department of Pharmacy, Universidad Nacional de Colombia, Bogotá, Colombia

ABSTRACT Transforming growth factor β (TGF-β) has been shown to play a role in immunity against different pathogens *in vitro* and against parasites *in vivo*. However, its role in viral infections *in vivo* is incompletely understood. Using a neonatal mouse model of heterologous rhesus rotavirus (RV) vaccination, we show that the vaccine induced rotavirus-specific CD4 T cells, the majority of which lacked expression of KLRG1 or CD127, and a few regulatory rotavirus-specific CD4 T cells that expressed surface latency-associated peptide (LAP)–TGF-β. In these mice, inhibiting TGF-β, with both a neutralizing antibody and an inhibitor of TGF-β receptor signaling (activin receptor-like kinase 5 inhibitor [ALK5i]), did not change the development or intensity of the mild diarrhea induced by the vaccine, the rotavirus-specific T cell response, or protection against a subsequent challenge with a murine EC-rotavirus. However, mice treated with anti-LAP antibodies had improved protection after a homologous EC-rotavirus challenge, compared with control rhesus rotavirus-immunized mice. Thus, oral vaccination with a heterologous rotavirus stimulates regulatory RV-specific CD4 LAP-positive (LAP$^+$) T cells, and depletion of LAP$^+$ cells increases vaccine-induced protection.

IMPORTANCE Despite the introduction of several live attenuated animal and human rotaviruses as efficient oral vaccines, rotaviruses continue to be the leading etiological agent for diarrhea mortality among children under 5 years of age worldwide. Improvement of these vaccines has been partially delayed because immunity to rotaviruses is incompletely understood. In the intestine (where rotavirus replicates), regulatory T cells that express latency-associated peptide (LAP) play a prominent role, which has been explored for many diseases but not specifically for infectious agents. In this paper, we show that neonatal mice given a live oral rotavirus vaccine develop rotavirus-specific LAP$^+$ T cells and that depletion of these cells improves the efficiency of the vaccine. These findings may prove useful for the design of strategies to improve rotavirus vaccines.

KEYWORDS neonatal mice, transforming growth factor β, intestine, latency-associated peptide, rotavirus, vaccine

Transforming growth factor beta (TGF-β) is a versatile cytokine that can promote different types of immune responses depending on the location and context in which it acts but is mainly tolerogenic and plays a critical role in intestinal immunity (1). Despite many *in vitro* studies that implicate TGF-β in immunity to pathogens, the *in vivo* role of this cytokine is incompletely understood (2). Several instances have been described in which parasites induce TGF-β and/or blocking of TGF-β ameliorates disease in animal models, implying that parasites use this cytokine/cytokine pathway to evade the

Citation Rey LM, Gil JÁ, Mateus J, Rodríguez L-S, Rondón MA, Ángel J, Franco MA. 2019. LAP$^+$ cells modulate protection induced by oral vaccination with rhesus rotavirus in a neonatal mouse model. J Virol 93:e00882-19. https://doi.org/10.1128/JVI.00882-19.

Editor Susana López, Instituto de Biotecnologia/UNAM

Copyright © 2019 American Society for Microbiology. All Rights Reserved.

Address correspondence to Manuel Antonio Franco, mafranco@javeriana.edu.co.

Received 6 June 2019
Accepted 9 July 2019
Accepted manuscript posted online 10 July 2019
Published 12 September 2019

Downloaded from http://jvi.asm.org/ on May 8, 2020 by guest

immune response (3). However, the situation is less clear against other pathogens and viruses in particular: in a model of chronic infection with lymphocytic choriomeningitis virus (LCMV), treatment of mice with an activin receptor-like kinase 5 inhibitor (ALK5i) (that blocks TGF-β receptor signaling) or administration of neutralizing antibodies against TGF-β failed to decrease viral replication, although it improved the antiviral T cell response (4, 5). In contrast, in mice acutely infected with influenza virus, systemic blocking of TGF-β with neutralizing antibodies promotes the development of the disease (6, 7). However, when TGF-β is directly or indirectly genetically inactivated in the lung epithelium of mice infected with influenza, the interferon beta (IFN-β) response is increased, and the mice are protected from developing severe pathology (8, 9). Thus, inhibiting TGF-β produced by lung epithelial cells early after infection, unlike systemic blocking of the cytokine, seems to inhibit influenza virus replication and disease, and further studies to understand the role of this cytokine in viral immunity *in vivo* are needed.

TGF-β1 is synthesized as a precursor composed of a signal peptide, a C-terminal fragment (the mature cytokine), and an N-terminal portion called latency-associated peptide (LAP), which surrounds the cytokine and forms a structure called the small latency complex (1). The expression of the LAP–TGF-β complex on CD4 T cells identifies a population of regulatory T cells (Treg) that play an important role in mucosal immunity and in particular in oral tolerance (10). These Treg depend on TGF-β for their generation and mediate tolerance in a TGF-β-dependent mechanism (10). The administration to mice of antibodies against LAP that deplete LAP-positive (LAP^+) Treg has been illuminating in establishing that these cells play a role in oral tolerance, autoimmune diseases, and antitumor immunity (11–15). To our knowledge, the role of LAP^+ cells in *in vivo* immunity to pathogens, and viruses in particular, using this strategy has not been evaluated.

Despite the introduction of several live attenuated animal and human rotaviruses (RVs) as efficient oral vaccines, RVs continue to be the leading etiological agent for diarrhea mortality among children under 5 years of age worldwide (16). Improvement of these vaccines has been partially delayed because immunity to RV is incompletely understood (17, 18). Our studies in children and adults infected with RV showed that RV-specific T cells (RV-T cells) circulate at frequencies below detection levels or at low frequencies (19) and have a poor functional profile (20), suggesting that RV has developed mechanisms to evade the immune response. Moreover, we have shown that *in vitro*, Caco-2 cells (a human intestinal cell line used as a model of the intestinal barrier) infected with RV secrete TGF-β1 and other nonproinflammatory cytokines, suggesting that RV may induce this cytokine to evade the immune response (21, 22).

We and others have shown that, in mice, CD8 T cells are involved in RV clearance and that antibodies (most of them dependent on CD4 T cell help) are the principal mechanisms that mediate protection against reinfection (23, 24). RV-T cells produced by infection of adult and neonatal mice with a heterologous rhesus RV (RRV) or with a homologous murine RV (EC-RV) are transiently detectable at low frequencies (25). These cells are identified with an intracellular cytokine assay after *in vitro* stimulation with peptides corresponding to several CD4 and CD8 T cell epitopes (25). Adult mice have, as expected, a high T cell response and different kinetics of response compared with neonates, but in both, surprisingly, the liver was the organ in which the highest numbers of RV-T cells were detected (25). Protection of neonatal BALB/c mice after vaccination with RRV, followed by challenge weeks later with a murine RV (probably the model that best reflects the human situation with human live oral vaccines), depends on antibodies (26). In this model, the dose of RRV used to generate protection triggers low levels of diarrhea, and protection is evaluated by measuring the quantity of viral antigen shed in feces, because mice become resistant to RV-induced diarrheal disease at 14 days of age (27).

In the present study, we evaluated, in neonatal mice orally vaccinated with RRV, whether the low levels of diarrhea prompted by the vaccine, the T cell and antibody responses, and the levels of protection varied in mice left untreated or treated with

Downloaded from http://jvi.asm.org/ on May 8, 2020 by guest

neutralizing antibodies to TGF-β or to LAP or with an ALK5i. We observed that pretreatment with RRV induced RV-CD4 T cells, the majority of which lacked expression of KLRG1 or CD127, and a few of them (~10%) expressed LAP. Moreover, mice treated with anti-LAP antibody, unlike those treated with anti-TGF-β antibody or ALK5i, had improved protection after challenge with a homologous murine EC-RV, compared with vaccinated mice treated with control preparations. Thus, depletion of LAP$^+$ cells increased the protection induced by a live oral RV vaccine.

RESULTS

Lack of modulation of RRV-induced diarrhea by treatment with anti-TGF-β or anti-LAP antibodies or with ALK5i. Contrary to human infants, for whom the first human RV infection usually fails to induce protection, neonatal mice infected with homologous wild-type RV, but not with heterologous RV, are protected after the first infection (26, 28). For this reason, oral infection of neonatal mice with 10^6 focus-forming units (FFU) of a heterologous RRV and subsequent challenge with a homologous wild-type RV have been used to model human RV vaccines (26, 28). However, unlike with human vaccination, RRV-infected mice develop mild diarrhea. Moreover, since at the time of challenge with wild-type RV, mice are too old to develop diarrhea, protection is measured by assessing viral excretion. Although imperfect, this is the best mouse model for studying RV vaccine protection and thus is used in the present report.

To determine the role of TGF-β and LAP$^+$ cells in the neonatal mouse model of RRV vaccination, suckling mice were vaccinated with RRV and treated with anti-LAP or anti-TGF-β monoclonal antibodies, an isotype control antibody (as a negative control), an ALK5i, or dimethyl sulfoxide (DMSO) (the diluent of ALK5i, used as a negative control), as described in Materials and Methods. First, the effect of these treatments on diarrhea induced by RRV was evaluated. Nonvaccinated mice were included as controls, and as expected, diarrhea was not detected in this group (Fig. 1). In the groups of mice vaccinated with RRV and treated with anti-TGF-β antibody, anti-LAP antibody, or the ALK5i, the frequency of mice that developed diarrhea on a daily basis (Fig. 1A and C) and the diarrhea intensity scores were comparable to those of vaccinated mice treated with isotype control antibody or DMSO (Fig. 1B and D). Thus, none of the treatments used to modulate TGF-β and LAP$^+$ cells (anti-TGF-β or anti-LAP antibodies or ALK5i) modified the symptoms induced by RRV vaccination.

RRV vaccination induces RV-CD4 and RV-CD8 T cells in spleen and liver, detectable with H-2 I-A^b and H-2K^b tetramers, which are unmodulated by anti-TGF-β or anti-LAP antibodies. Frequencies of epitope-specific RV-CD4 and RV-CD8 T cells have been assessed in the past with an intracellular cytokine assay (25) or with class I tetramers (29). To determine if frequencies of total and RV-T cells were modified in mice vaccinated with RRV and treated with anti-TGF-β or anti-LAP antibodies, we stained liver lymphocytes and splenocytes with a class I H-2K^b RV VP7$_{33-40}$ tetramer (25), a class II I-A^b RV VP6$_{245-259}$ tetramer (25), or a control class II I-A^b human CLIP$_{87-101}$ tetramer and used the corresponding peptides to stimulate splenocytes in an intracellular cytokine assay. Splenocytes and liver lymphocytes were isolated 12 days after vaccination with RRV and before challenge with murine EC-RV, to assess the immune response that developed prior to challenge. The strategy to analyze the frequencies of total and tetramer-positive T cells is presented in Fig. S1 in the supplemental material.

In the spleen, the frequencies of total CD4 T cells were lower, and those of CD8 T cells were higher, in RRV-vaccinated mice treated with the antibodies than in nonvaccinated animals, especially for anti-TGF-β-treated mice (Fig. 2A and D). A similar trend was observed for CD8 T cells in liver (Fig. 3A and D).

RV-CD4 and RV-CD8 T cells were detected with the tetramers at low frequencies (less than 1%) in all RRV-immunized groups treated with isotype control, anti-TGF-β, or anti-LAP antibodies, in both spleen (Fig. 2B and C) and liver (Fig. 3B and C) and were not statistically different between any of the groups of mice that received antibody treatments.

Downloaded from http://jvi.asm.org/ on May 8, 2020 by guest

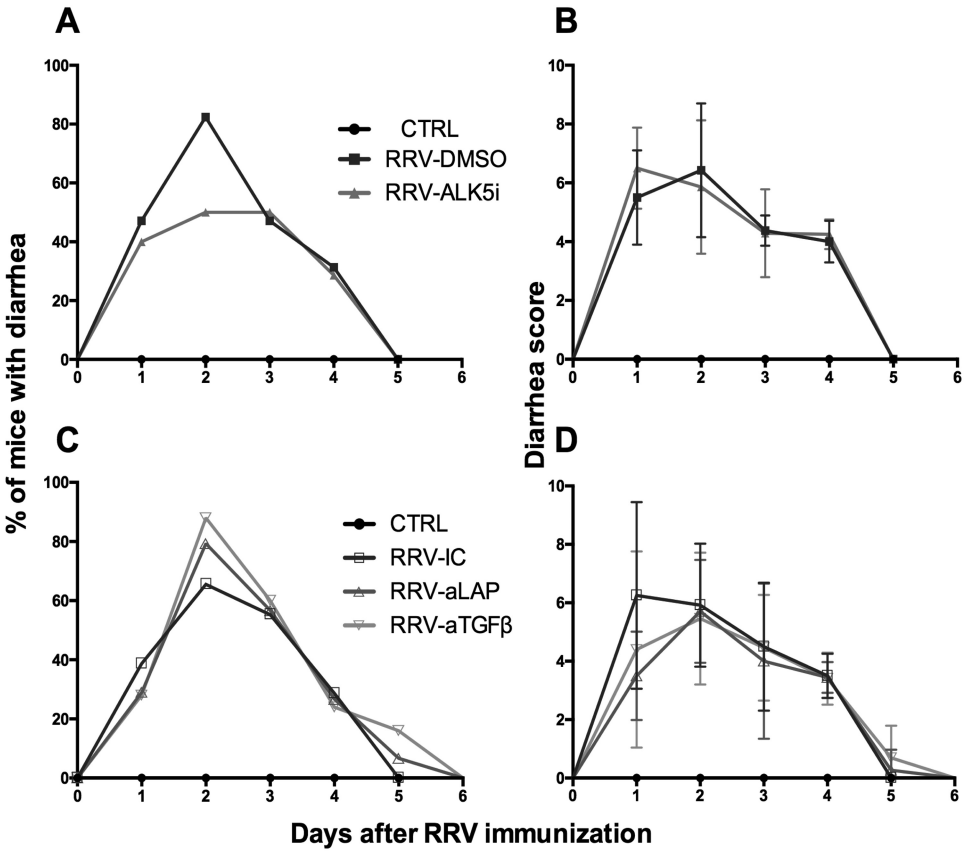


FIG 1 Diarrhea frequency and intensity in mice vaccinated with RRV. For diarrhea intensity, the average scores for mice with the corresponding day after infection are shown. (A and B) Experiments with ALK5i; (C and D) experiments with antibodies against TGF-β or LAP. CTRL indicates mock-immunized animals, and RRV-DMSO, RRV-ALK5i, RRV-IC, RRV-aLAP, and RRV-aTGFβ are mice vaccinated and treated with ALK5i diluent, ALK5i, isotype control antibody, anti-LAP, and anti-TGF-β, respectively. Results in panels A and B are pooled from 2 experiments, and those in panels C and D are pooled from 4 experiments, with 6 to 9 mice per group in each experiment. No statistically significant differences were noted between study groups in any of the experiments presented.

In two independent experiments, total and RV-T cells from mice vaccinated and receiving ALK5i or its diluent (DMSO) were found at similar frequencies (data not shown).

To quantify functional RV-T cells, we used an intracellular cytokine assay with splenocytes of control or vaccinated mice that received the different treatments, as previously described (25). Frequencies of IFN-γ-positive (IFN-γ^+) T cells that were low or below the level of detection of the assay were identified in response to the class II-restricted $VP6_{245-259}$ and class I-restricted $VP7_{33-42}$ peptides or to RRV (data not shown). Frequencies of interleukin-2 (IL-2)-, tumor necrosis factor alpha (TNF-α)-, or IL-10-producing T cells in response to all stimuli were below the level of detection of the assay (data not shown).

In conclusion, RV-CD4 and RV-CD8 T cells were detected at low frequencies after RRV vaccination, and modulation of these responses with anti-TGF-β or anti-LAP was not observed.

RV-CD4 and RV-CD8 T cells are enriched in KLRG1$^-$/CD127$^-$ and KLRG1$^-$/CD127$^+$ subsets, respectively. Next, we examined the differentiation stage of RV-T memory cells induced after RRV vaccination. For CD8 memory (CD44$^+$) T cells, KLRG1 and CD127 markers identify early effector cells (EEC) (KLRG1$^-$/CD127$^-$), memory precursor effector cells (MPEC) (KLRG1$^-$/CD127$^+$), and short-lived effector cells (SLEC) (KLRG1$^+$/CD127$^-$) (30–32). For CD4 T cells, a classification based on these markers is less well established, and we refer to these cells based on the expression of these

Downloaded from http://jvi.asm.org/ on May 8, 2020 by guest

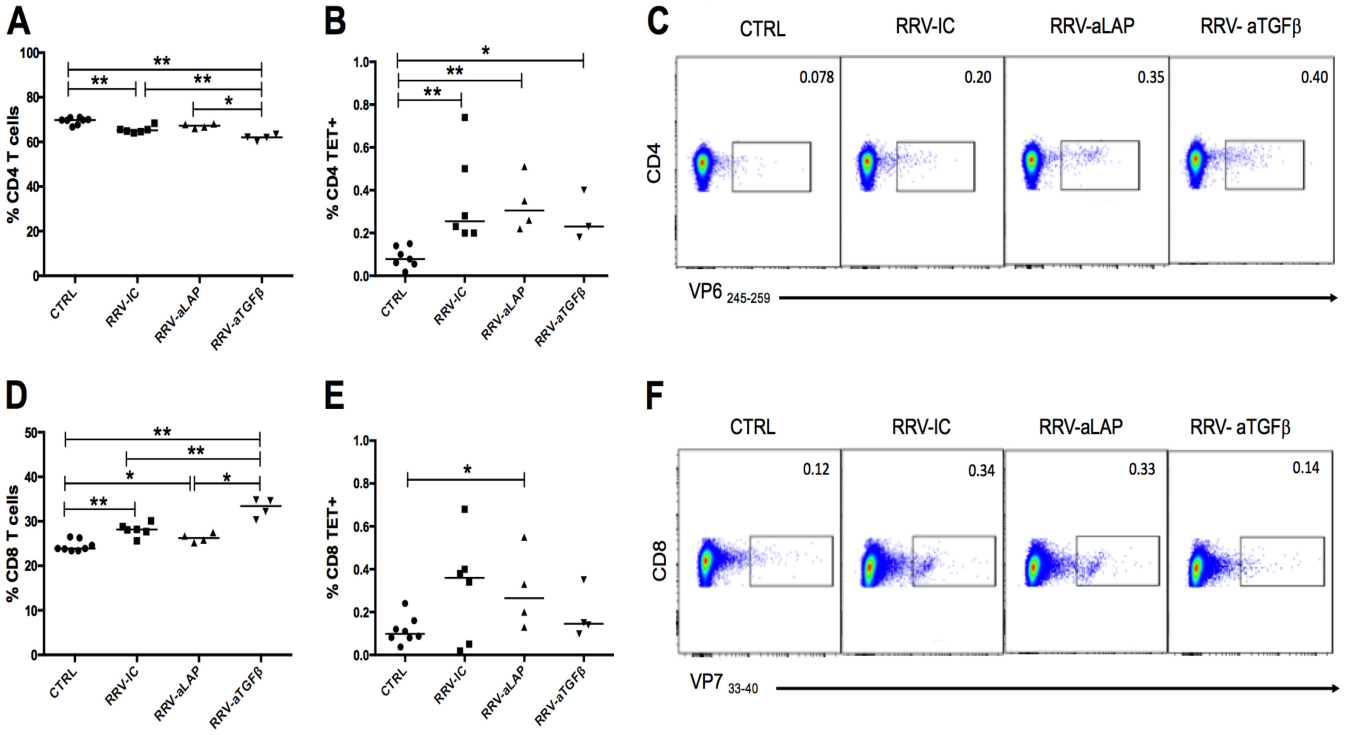


FIG 2 RV-specific T cell responses in spleen. Fresh splenocytes were harvested 12 days after oral RRV vaccination and stained to identify CD4 or CD8 T cells and class I or II tetramer-positive T cells by flow cytometry. (A, B, D, and E) Frequencies of total and RV-CD4 and RV-CD8 T cells; (C and F) representative dot plots of CD4 tetramer-positive or CD8 tetramer-positive T cells. The full analysis strategy for these experiments is presented in Fig. S1 in the supplemental material. Each point represents results with cells from 1 to 3 animals that were pooled for each of 4 experiments performed. The control class II I-A^b human $CLIP_{87–101}$ tetramer stained T cells from vaccinated mice at frequencies comparable to those shown for control nonvaccinated mice (data not shown). Lines in graphs represent the medians for each group. *, $P < 0.05$; **, $P < 0.01$ (by a Mann-Whitney test).

markers (33, 34). To evaluate the phenotypes of total and RV-T cells modulated by vaccination and the different antibody treatments, we included these three markers in the tetramer staining panel, as described in Materials and Methods.

In both spleen (Fig. 4A to D) and liver (Fig. 4E to H), most total CD4 T cells were KLRG1$^-$/CD127$^-$, and the majority of total CD8 T cells were KLRG1$^-$/CD127$^+$ (MPEC) in all groups of mice.

In spleen, in response to RRV vaccination, total frequencies of CD4 KLRG1$^-$/CD127$^-$ cells increased in anti-LAP-treated mice (Fig. 4A), compared with control nonvaccinated mice. In contrast, total KLRG1$^-$/CD127$^+$ frequencies of CD8 T cells in spleen decreased in RRV-immunized mice treated with the isotype control, anti-LAP, and anti-TGF-β, compared with control mice (Fig. 4B).

To determine if, compared to total T cells, RV-T cells were enriched in cells of a particular phenotype, we compared frequencies of RV-CD4 (Fig. 4C) or RV-CD8 (Fig. 4D) T cells from all RRV-vaccinated animals with the corresponding total CD4 or CD8 T cells (Fig. 4C and D). In spleen, while RV-CD4 T cells were enriched in KLRG1$^-$/CD127$^-$ cells (Fig. 4C), a lack of enrichment of RV-CD8 T cells in KLRG1$^-$/CD127$^+$ cells was detected (Fig. 4D). In liver, the vaccinated mice that received the isotype control antibody and anti-TGF-β had significantly lower percentages of total CD4 KLRG1$^-$/CD127$^-$ T cells than control mice (Fig. 4E), and frequencies of total CD8 KLRG1$^-$/CD127$^+$ populations were similar in all groups (Fig. 4F). Liver RV-CD4 T cells and RV-CD8 T cells were enriched in KLRG1$^-$/CD127$^-$ and KLRG1$^-$/CD127$^+$ cells, respectively, when they were compared with total CD4 or CD8 T cells (Fig. 4G and H).

In conclusion, when T cells from all RRV-vaccinated mice were analyzed together, RV-CD4 T cells were enriched in KLRG1$^-$/CD127$^-$ cells in both spleen and liver, while RV-CD8 T cells were enriched in KLRG1$^-$/CD127$^+$ cells (MPEC) in the liver but not in the spleen.

Downloaded from http://jvi.asm.org/ on May 8, 2020 by guest

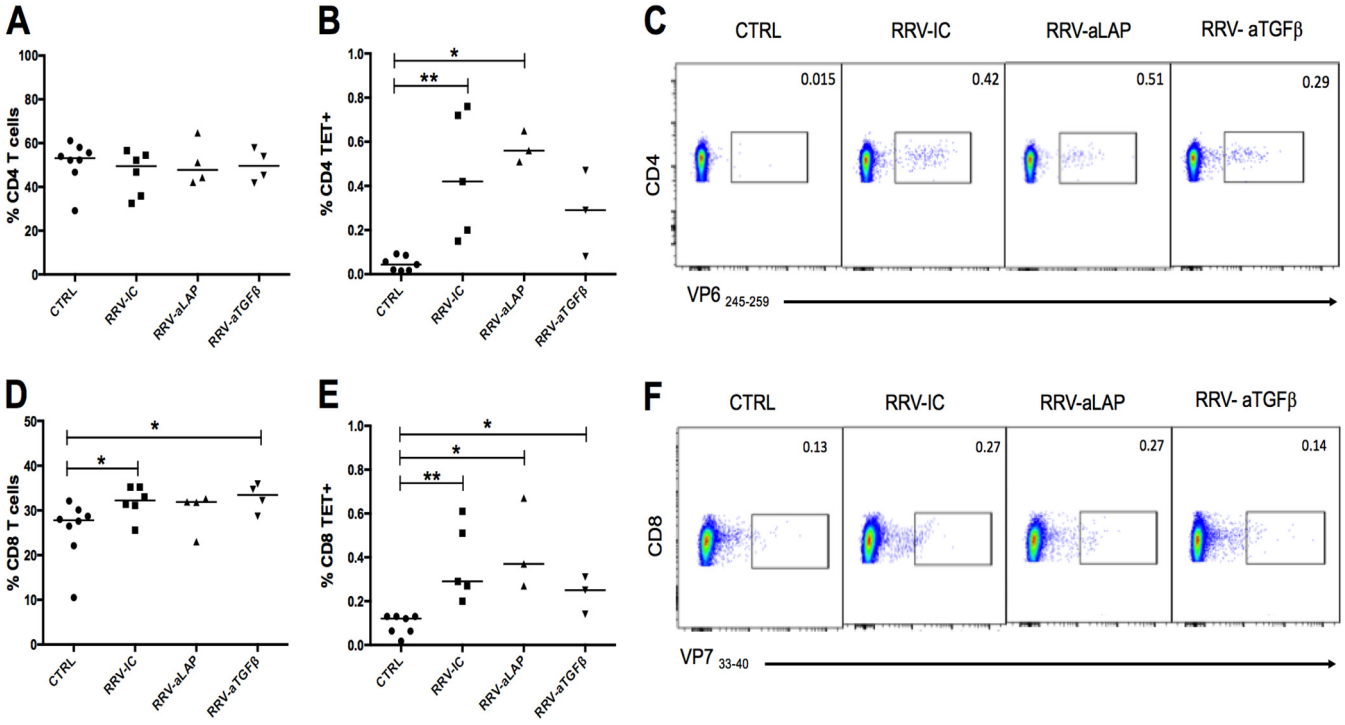


FIG 3 RV-specific T cell response in liver. Fresh mononuclear cells from the liver were harvested 12 days after oral RRV vaccination and stained to identify CD4 and CD8 T cells and class I or II tetramer-positive T cells by flow cytometry. (A, B, D, and E) Frequencies of total and RV-CD4 and RV-CD8 T cells; (C and F) representative dot plots of CD4 tetramer-positive or CD8 tetramer-positive T cells. Cells from 1 to 3 animals were pooled for each of 4 experiments performed. The control class II I-A^b human $CLIP_{87-101}$ tetramer stained T cells from vaccinated mice at frequencies comparable to those shown for control nonvaccinated mice (data not shown). Lines in graphs represent the medians for each group. *, $P < 0.05$; **, $P < 0.01$ (by a Mann-Whitney test).

RRV vaccination reduces the frequency of total memory ($CD44^+$) LAP^+ cells in spleen and induces CD4 tetramer-positive LAP^+ T cells in spleen and liver. As stated above, LAP^+ Treg play an important role in mucosal immunity, and they can be depleted in mice by the administration of antibodies against LAP (11–15). First, we verified if anti-LAP antibody treatment effectively depleted total CD4 LAP^+ T cells. In spleen, as expected, splenocytes of anti-LAP-treated mice had a 4-fold decrease in total CD4 LAP^+ T cells (Fig. 5A) compared with nonvaccinated mice, isotype control-treated mice, or anti-TGF-β antibody-treated mice. When CD4 $CD44^+$ LAP^+ memory T cells were analyzed, this difference was even more pronounced (10-fold decrease) in spleens of anti-LAP-treated mice (Fig. 5B). A small, but statistically significant, reduction in CD4 $CD44^+$ LAP^+ memory T cells in isotype control antibody- and anti-TGF-β-treated mice with respect to control nonvaccinated mice was detected, implying that RRV vaccination diminished CD4 LAP^+ Treg in spleen (Fig. 5B). In liver, a non-statistically significant tendency of total CD4 LAP^+ T cells to be decreased was seen in anti-LAP-treated mice (Fig. 5D), and percentages of CD4 $CD44^+$ LAP^+ memory T cells of anti-LAP-treated mice declined, with statistical significance (Fig. 5E).

RRV vaccination induced CD4-RV LAP^+ T cells in both spleen and liver at median frequencies of 9.5% (Fig. 5C and F). The frequency of CD4-RV LAP^+ T cells was lower (with statistical significance) than that of their corresponding total CD4 LAP^+ T cells (Fig. 5C) in spleen but not liver (Fig. 5F).

The effect of anti-TGF-β was also verified, and, as expected, mice treated with anti-TGF-β (but not those treated with anti-LAP antibody) had a significant ($P < 0.0003$) 7.4-fold decrease in median levels of total (acid-activated) TGF-β in serum, compared with isotype control-treated mice 12 days after vaccination (data not shown).

In conclusion, biological effects of both anti-LAP and anti-TGF-β antibodies in treated mice were observed, and RRV vaccination induced CD4-RV LAP^+ T cells in both spleen and liver.

Downloaded from http://jvi.asm.org/ on May 8, 2020 by guest

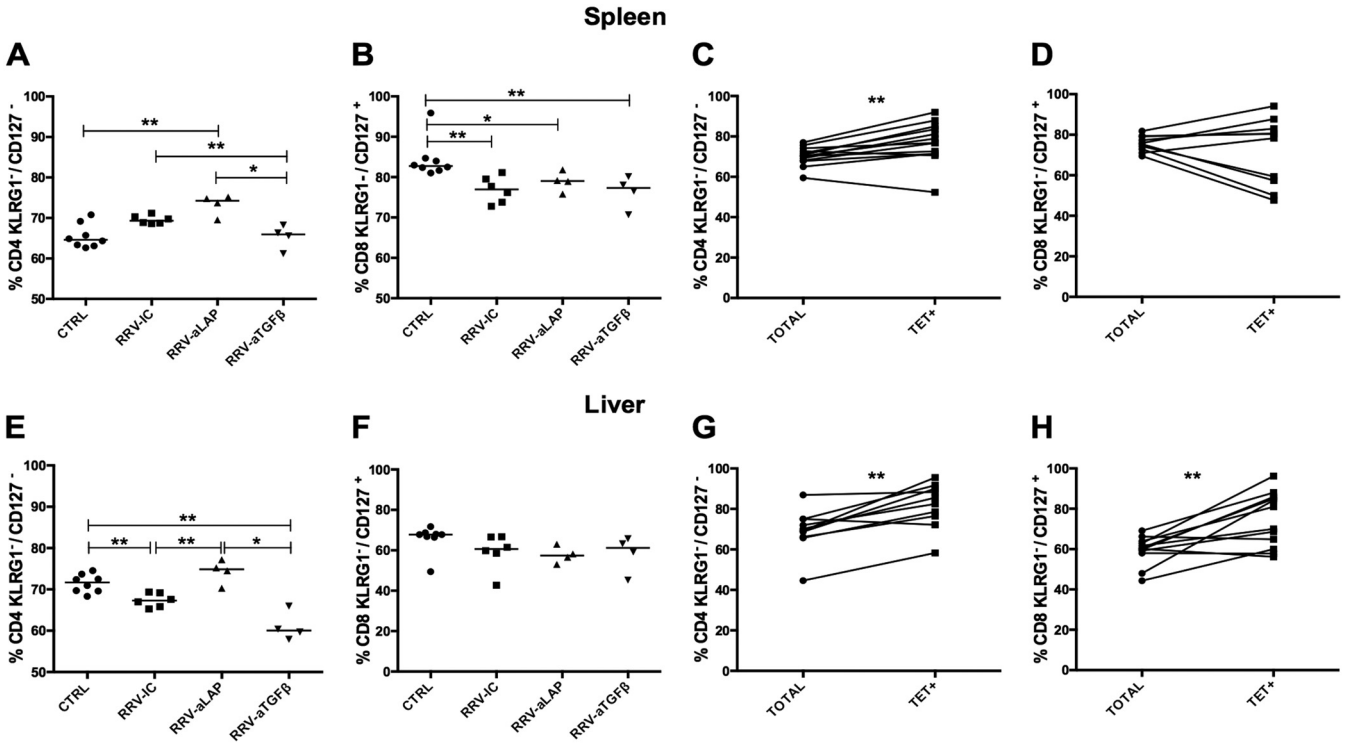


FIG 4 Frequencies of KLRG1$^-$/CD127$^-$ and KLRG1$^-$/CD127$^+$ T cells in spleen and liver. Frequencies of KLRG1$^-$/CD127$^-$ and KLRG1$^-$/CD127$^+$ cells were determined for CD4 or CD8 CD44$^+$ T cells. (A, B, E, and F) Frequencies of total KLRG1$^-$/CD127$^-$ and KLRG1$^-$/CD127$^+$ T cells; (C, D, G, and H) comparison between frequencies of total and RV-T cells in groups where KLRG1$^-$/CD127$^-$ and KLRG1$^-$/CD127$^+$ populations were detected. The latter graphs include T cells from two vaccinated mice that received ALK5i. Cells from 1 to 3 animals were pooled for each of 4 experiments performed. Lines in graphs represent the medians for each group. *, $P < 0.05$; **, $P < 0.01$ (by a Mann-Whitney test [A, B, E, and F] or a Wilcoxon test [C, D, G, and H]). TET+, tetramer positive.

Depletion of LAP$^+$ cells improves RRV-induced protection against RV. Finally, we assessed the degree of protection induced by oral RRV vaccination in mice treated or not treated with anti-TGF-β, anti-LAP, or ALK5i. For this purpose, all groups of mice (nonvaccinated and vaccinated) were challenged with wild-type EC-RV at day 12 after vaccination with RRV, and antigen viral shedding was measured from day 0 of EC-RV challenge to day 10 after challenge. Compared with nonvaccinated mice, all groups of RRV-vaccinated mice shed small amounts of antigen after challenge (Table 1 and Fig. 6A and B) and for a low number of days ("delayed clearance"; $P < 0.0001$). Mice that received ALK5i exhibited a similar antigen shedding curve as mice treated with DMSO (Fig. 6A), and the same was observed for anti-TGF-β-treated mice with respect to the isotype control group (Fig. 6B and Table 1), indicating that ALK5i and anti-TGF-β treatments failed to improve protection. In contrast, mice depleted of LAP$^+$ cells were more protected because they shed lower quantities of antigen than the isotype control- and anti-TGF-β-treated groups, and the relative risk for shedding virus was statistically significantly lower than for isotype control- and anti-TGF-β-treated mice (Fig. 6B and Table 1).

Since it was previously shown that in this "neonatal mouse model for active protection studies with RV vaccines," protection was mediated by antibodies (26), the level of RV-IgA in stool was measured. On the day of challenge (day 12 after RRV vaccination), all groups of vaccinated mice had low or below-detection levels of RV-IgA in their stool samples (data not shown). On day 10 after challenge, all vaccinated mice had higher levels of RV-IgA than control nonvaccinated mice (Fig. 6C and D), and the anti-LAP-treated group had statistically significantly higher median levels of RV-IgA than the anti-TGF-β group (Fig. 6D).

In conclusion, mice vaccinated with heterologous RV and depleted of LAP$^+$ T cells were more protected against homologous RV challenge than control mice and developed high titers of RV-IgA.

Downloaded from http://jvi.asm.org/ on May 8, 2020 by guest

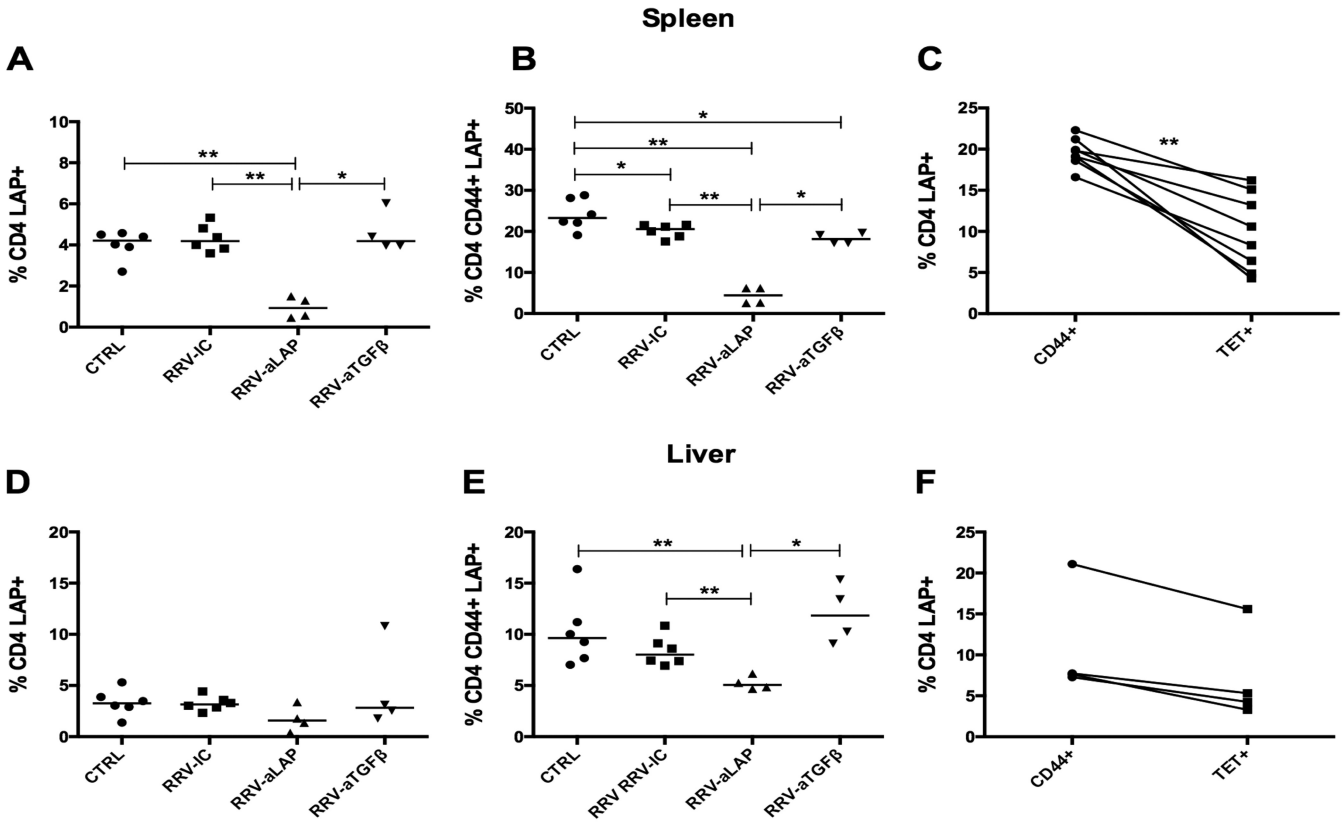


FIG 5 Total CD4 LAP$^+$ T cells in spleen and liver are depleted by anti-LAP treatment, and RV-CD4 LAP$^+$ T cells induced by vaccination are present at frequencies similar to or lower than those of total CD4 LAP$^+$ T cells. Fresh mononuclear cells from the spleen and liver were harvested 12 days after oral RRV vaccination and stained to identify CD4 LAP$^+$ T cells by flow cytometry. (A and D) Frequency of total CD4 LAP$^+$ T cells; (B and E) frequency of total CD4 CD44$^+$ LAP$^+$ T cells; (C and F) comparison between frequencies of total CD4 CD44$^+$ LAP$^+$ T cells and frequencies of RV-CD4 CD44$^+$ LAP$^+$ T cells from spleen and liver. The latter graphs include T cells from two vaccinated mice that received ALK5i, and in the case of liver T cells, some tetramer-positive cells were not included because fewer than 5 LAP$^+$ events (level of detection determined for the flow cytometry experiments) were detectable. Cells from 1 to 3 animals were pooled for each of 4 experiments performed. Lines in graphs represent the medians for each group. *, $P < 0.05$; **, $P < 0.01$ (by a Mann-Whitney test [A, B, D, and E] or a Wilcoxon test [C and F]).

DISCUSSION

Here, we used what we consider the best mouse model to assess the mechanisms of protection generated by RV vaccines (26, 28). We found that oral vaccination of neonatal C57BL/6 mice with 10^6 FFU of RRV provoked partial (~50%) (Table 1) protection against challenge with murine EC-RV. Vaccination induced RV-CD4 LAP$^+$ T cells (a Treg phenotype), and depletion of these cells by administration of a specific antibody improved vaccine-induced protection. To our knowledge, this is the first time

TABLE 1 Protection after EC-RV challenge

Treatment	No. of mice	Mean quantity of antigen shed (SD_{50}/mouse/day) ± SD[a]	% protection[b]	Avg risk (95% confidence interval)
Mock	18	542,383 ± 2,325		
RRV-IC[c]	16	254,135 ± 1,151	53.1	5.58 (5.48–5.68)
RRV–anti-LAP	15	178,096 ± 1,779	67.2	5.38 (5.26–5.51)[d]
RRV–anti-TGF-β	16	270,364 ± 1,736	50.2	5.61 (5.49–5.72)

[a]Mean quantity of RV antigen shed ± standard deviation over 10 days postchallenge. Numbers are the cumulative results from three independent experiments.
[b]Percent protection is the percent decrease in the mean quantity of RV antigen shed during the 10 days after challenge, compared with that of mock-treated mice.
[c]IC, isotype control antibody.
[d]Significantly ($P < 0.03$) lower than for RRV-IC.

Downloaded from http://jvi.asm.org/ on May 8, 2020 by guest

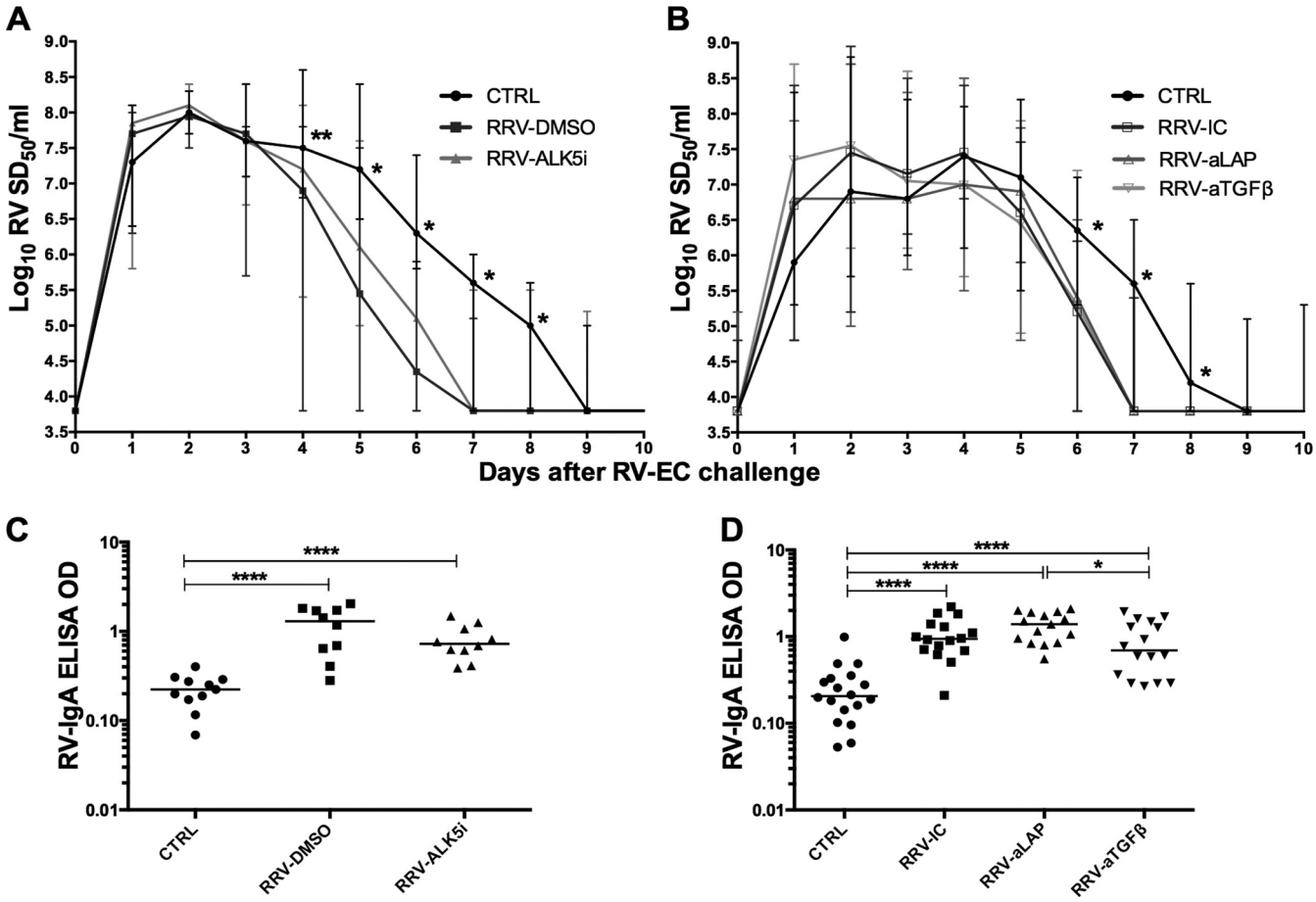


FIG 6 Fecal RV antigen curve and virus-specific intestinal IgA after EC-RV challenge. At day 12 postimmunization, RRV- or mock-vaccinated mice were challenged with 10^5 SD_{50} of homologous EC-RV to evaluate protection. Fecal pellets were collected every day and analyzed for the presence of antigen and RV-IgA by an ELISA. (A and B) Results are shown as the medians and ranges for the group for each day after EC-RV challenge. **, $P = 0.0052$ between control (CTRL) and DMSO-treated mice (for panel A) (by a Mann-Whitney test); *, $P < 0.002$ between control and all other groups (for both panels A and B) (by a Mann-Whitney test). (C and D) Each symbol represents RV-IgA (ELISA OD) present in the stool of an individual mouse at day 10 of challenge. The horizontal line indicates the median for each group. *, $P < 0.05$; ****, $P < 0.001$ (by a Mann Whitney test). Pooled results from 2 experiments (A and C) or 3 experiments (B and D) with 4 to 7 mice per group are shown.

that administration of an antibody against LAP+ cells has been shown to modulate protection after vaccination against a pathogen *in vivo*.

Previous *ex vivo* experiments with peripheral blood mononuclear cells (PBMC) of healthy humans and *in vitro* experiments with Caco-2 cells in our group suggested that RV may induce TGF-β to evade the immune response (21, 22). Here, we studied the *in vivo* role of TGF-β and LAP+ cells in diarrhea induced by heterologous RRV vaccination (Fig. 1). We found that treatment with anti-TGF-β or anti-LAP or inhibition of TGF-β signaling with ALK5i did not modulate the frequencies and intensities of diarrhea provoked by RRV oral infection (Fig. 1). These results are in agreement with previous *in vitro* studies showing that although TGF-β increased during RV infection, it failed to produce the expected enterocyte apoptosis, because of concomitant stimulation of microRNA miR-142-5p that inhibits this apoptosis (35). Thus, TGF-β may lack a net modulatory function at the level of the enterocyte during heterologous RV infection. Future studies are necessary to determine if RRV increases TGF-β levels in our model and to better understand why RRV-induced diarrhea in neonatal mice remains unmodified after blocking this cytokine.

Inhibiting TGF-β or eliminating LAP+ T cells failed to modulate the frequencies of RV-CD8 and RV-CD4 T cells, identified with class I and class II tetramers, generated by RRV infection in spleen and liver (Fig. 2B and E and Fig. 3B and E). However, the number

Downloaded from http://jvi.asm.org/ on May 8, 2020 by guest

of experiments performed to quantify these cells was low (3 to 4 in the case of antibody-treated animals), and further studies are needed to confirm this conclusion. These results appear opposed to findings with LCMV, where treatment of mice with the same neutralizing antibody against TGF-β or with a similar ALK5i increased the T cell response to LCMV (4, 5). Differences in the levels of viral replication and other variables can potentially explain this discrepancy. Notably, the levels of RV-T cells detected with the tetramers in spleen (Fig. 3B and E) are higher than those of T cells producing IFN-γ detected with an intracellular cytokine assay (data not shown), suggesting that some RV-T cells lack cytokine production and are in an anergic state. In addition, the fact that we detected RV-T cells producing only IFN-γ, but not IL-2 or TNF-α (data not shown), is in agreement with our studies in children, where most RV-T cells secrete only IFN-γ, and higher frequencies seem to be detectable using the tetramers than by the intracellular cytokine assay (20, 36). These findings support the hypothesis that in neonatal mice and children, RV may have developed mechanisms to evade the T cell immune response (2).

The predominant phenotypes of RV-CD4 and RV-CD8 T cells were KLRG1$^-$/CD127$^-$ and KLRG1$^-$/CD127$^+$ (MPEC), respectively (Fig. 4C, D, G, and H). At the peak of the response, infection with *Listeria monocytogenes* predominantly promotes the development of CD8 KLRG1$^+$/CD127$^-$ cells (SLEC), while similar infection with vesicular stomatitis virus (VSV), influenza virus, or vaccinia virus results in higher frequencies of KLRG1$^-$/CD127$^-$ cells (EEC) and KLRG1$^-$/CD127$^+$ cells (MPEC) (30, 37). Thus, RV-CD8 T cells phenotypically most closely resemble virus-induced CD8 T cells. The generation of KLRG1$^-$/CD127$^+$ (MPEC) RV-CD8 T cells (Fig. 4D and H) suggests that vaccination was efficient at inducing long-lived T cells with memory potential (31).

The induction of different subsets of Treg after RV infection and their role in protection have been addressed in mice and pigs (38–40). In pigs, frequencies of IL-10- and TGF-β-secreting CD4 CD25$^-$ FoxP3$^+$ Treg in the intestine were significantly inversely correlated with protection against RV diarrhea (38). Notwithstanding, in the mouse model, no role for FoxP3$^+$ CD25$^+$ Treg in RV infection and immunity has been evidenced (39, 40). Here, we have shown that since mice depleted of LAP$^+$ cells had a lower relative risk for shedding challenge EC-RV than isotype control- and anti-TGF-β-treated mice (Fig. 6B and Table 1), the few (9.5%) (Fig. 5C and F) vaccine-induced RV-CD4 LAP$^+$ Treg may play a role in downregulating protection induced by oral RRV vaccination. However, anti-LAP treatment has many other effects, such as increased cytotoxic T lymphocyte (CTL) responses, reduction of tolerogenic CD103$^+$ CD8 T cells, activation of NK cells, maturation of dendritic cells, and improved immune memory (11), and thus, the mechanism of enhanced protection against RV in our model is still uncertain.

Anti-TGF-β- and ALK5i-treated mice had levels of protection similar to those of control mice (Fig. 6A and B), implying that, contrary to our working hypothesis (2), TGF-β is an unlikely RV-induced mechanism to evade the immune response. However, this hypothesis cannot be completely ruled out because CD4 LAP$^+$ Treg that seem to be involved in protection against RV (Fig. 6B) depend on TGF-β for their development and exert their function via TGF-β (1).

In BALB/c neonatal mice, protection induced by RRV seems to be dependent on antibodies (26), but the mechanism of protection generated by RRV in neonatal C57BL/6 mice remains undetermined. In our experiments, all vaccinated mice had higher levels of fecal RV-IgA at 10 days postchallenge than control nonvaccinated mice (Fig. 6C and D), suggesting that these antibodies could also be mediating protection. However, RV-IgA was below levels of detection or at low levels before the challenge (data not shown) in all groups of mice, and thus, prechallenge IgA may be unnecessary for protection. Finally, it is noteworthy that the principal difference between the antigen shedding curves of nonvaccinated and vaccinated mice (Fig. 6A and B) was a delay in viral clearance. In mice, CD8 T cells mediate viral clearance (41), and thus, these cells may also be implicated in protection in our model. Future studies analyzing in more detail the effect of anti-LAP treatment on the RV-CD8 T cell and RV antibody

Downloaded from http://jvi.asm.org/ on May 8, 2020 by guest

responses (the two most likely effector mechanisms involved in the protective response in our model) may help clarify this mechanism.

In conclusion, we have shown that anti-LAP treatment enhances protection induced by an oral RV vaccine *in vivo*. Further studies are needed to determine if the mechanism of increased protection is the elimination of RV-CD4 LAP$^+$ Treg induced by the vaccine.

MATERIALS AND METHODS

Viruses. A tissue culture-adapted RRV strain of simian RV (G3, P[3]; obtained from H. B. Greenberg, Stanford University, CA) was grown, and titers were determined, on MA104 cells in the presence of trypsin and used after semipurification on a 40% sucrose gradient (42). The semipurified stock virus preparation had a titer of 10^9 focus-forming units (FFU)/ml. For T cell stimulation and RV-specific IgA (RV-IgA) enzyme-linked immunosorbent assays (ELISAs), supernatants of RRV- or mock-infected MA104 cells (mock) were used. Stocks of wild-type murine RV (EC) were prepared as intestinal homogenates, and their titers, expressed as 50% shedding doses (SD_{50}), were determined in 12-day-old mice, as previously described (43). SD_{50} is the dose at which 50% of animals shed viral antigen, which for the EC strain of RV is the same as the DD_{50} (dose at which 50% of neonatal mice develop diarrhea) (27).

Mice and RRV immunization. C57BL/6 mice were originally purchased from Charles River (Wilmington, MA) and bred in our facility under specific-pathogen-free (SPF) conditions. Neonatal mice received 1×10^6 FFU of RRV in 50 μl or received 50 μl of mock administered by oral gavage at between 5 and 7 days of age. The presence or absence of diarrhea was evaluated in each animal up to 5 days after RRV immunization by applying gentle pressure to the abdomen (24). The severity of diarrhea was scored daily by assigning numeric values to the color, degree of soiling, and consistency of the stool, as previously described (26), and scoring was performed by an examiner who was blind to the treatment received by the animal (26). Mock-treated or RRV-immunized mice were challenged with 10^5 SD_{50}/50 μl of the murine EC-RV strain. Fecal samples were collected from each mouse on the day of challenge and for the 10 following days. Samples were stored frozen at −20°C until used for ELISAs. All procedures were performed in accordance with a protocol reviewed and approved by the Institutional Animal Care and Use Committee (IACUC). The animal facility and IACUC carry out their activities according to the *Guide for the Care and Use of Laboratory Animals*, 8th ed. (44), and performed postapproval monitoring.

Administration of antibodies to TGF-β and LAP and an ALK5i. Neonatal mice were injected intraperitoneally (i.p.) with 1.3 μg/g (host weight) of anti-LAP antibody (clone TW7-20B9; BioLegend, San Diego, CA, USA) (12), 87 μg/g of the neutralizing anti-TGF-β antibody (clone 1D11.16.8; BioXCell, West Lebanon, NH, USA), or the mouse IgG1 isotype control antibody (BioXCell, West Lebanon, NH, USA) (45) starting the day before RRV immunization and every other day for 12 days. SB 431542 (Sigma-Aldrich, St. Louis, MO, USA), an ALK5i, was administered i.p. at a dose of 17.3 μg/g (46) as a solution with 10% (vol/vol) DMSO and with the same inhibition scheme as the one described above. As additional controls, mice were inoculated with 50 μl of 10% (vol/vol) DMSO.

Flow cytometry analysis. Spleen and liver mononuclear cells were harvested 12 days after vaccination using previously described protocols (24, 25). For each experiment, 1 to 3 livers or 1 to 3 spleens of mice of the same treatment groups were pooled to obtain enough cells for the studies. Liver-infiltrating lymphocytes were isolated by mechanical disruption through a wire mesh and isolation of the lymphocytes on a 33% Percoll gradient (25). To identify RV-T cells, mononuclear cells from the spleen and liver were stained for 1 h at 4°C with the H-2K^b murine RV $VP7_{33-40}$ (IVYRFLFV) phycoerythrin (PE)-labeled tetramer (25) or for 2 h at room temperature with the class II I-A^b RV $VP6_{245-259}$ (ATWYFNPVILRPNNV) PE-labeled tetramer (25) or with a control class II I-A^b human $CLIP_{87-101}$ (PVSKMRMATPLLMQA) tetramer, all provided by the NIH Tetramer Core Facility. Subsequently, 10^6 cells were stained with Aqua diluted 1:40 in phosphate-buffered saline (PBS) and incubated for 20 min at room temperature. Previously titrated antibodies against CD3 peridinin chlorophyll protein (PerCP)-Cy5.5 (clone 17A2), CD4 Alexa Fluor 700 (AF700) (clone RM4-5), CD8a allophycocyanin (APC)-H7 (clone 53-6.7), and CD44 APC (clone IM7) were purchased from BD Biosciences (San Jose, CA, USA). Anti-CD127 PE-Cy7 (clone A7R34) and anti-KLRG1 fluorescein isothiocyanate (FITC) (clone 2F1; purchased from eBioscience, San Diego, CA, USA) and an anti-LAP BV421 antibody (clone TW7-16B4; purchased from BioLegend San Diego, CA, USA) were also included. All cells were fixed in cold PBS with 1% paraformaldehyde.

To quantify RV-T cells with an intracellular cytokine staining assay, splenocytes were stimulated for 6 h at 37°C in 5% CO_2 with 2 μg/ml peptides corresponding to class I-restricted ($VP7_{33-40}$), class II-restricted ($VP6_{245-259}$), or class II-restricted ($CLIP_{87-101}$ [control]) epitopes or stimulated with RRV or mock in the presence of 100 U/ml recombinant IL-2 (Chiron, Emeryville, CA), and 10 μg/ml of brefeldin A (Sigma-Aldrich, St. Louis, MO, USA) (25) was added 1 h later. Following 5 h of *in vitro* stimulation, cells were incubated with rat anti-mouse CD16/CD32 (clone 2.4G2; BD Biosciences, San Jose, CA, USA) for 5 min at 4°C to block Fc receptors; stained for Aqua CD3, CD4, and CD8 (as described above); and then fixed and permeabilized with Cytofix/Cytoperm and Permwash buffer (both from BD Biosciences, San Jose, CA, USA). Cells were then stained with antibodies against IFN-γ FITC (clone XMG1.2), IL-2 BV421 (clone JES65-H4), TNF-α PE-Cy7 (clone MP6-XT22), and IL-10 PE (clone JES5-16E3) (all from BD Biosciences, San Jose, CA, USA). Cells were acquired on a FACSAria IIup flow cytometer (BD Biosciences, San Jose, CA, USA), and data were analyzed with FlowJo software (TriStar, San Carlos, CA, USA).

Detection of viral antigen and RV-IgA by an ELISA. For detection of viral antigen in fecal samples, 96-well polystyrene flat-bottom microtiter plates (Thermo Fisher, Waltham, MA, USA) were coated with a 1:8,000 dilution (in PBS) of rabbit anti-RV antiserum (Dako, Denmark) and incubated overnight at 4°C. The plates were then blocked with 5% BLOTTO (5% [wt/vol] powdered milk in PBS with 0.1% Tween 20)

Downloaded from http://jvi.asm.org/ on May 8, 2020 by guest

at 37°C for at least 30 min. Ten percent (wt/vol) stool suspensions were prepared with PBS and 1% protease inhibitor cocktail containing 4-(2-aminoethyl)benzenesulfonyl fluoride hydrochloride (AEBSF), aprotinin, bestatin, E-64, leupeptin, and pepstatin A (Sigma-Aldrich, St. Louis, MO, USA); diluted in 5% BLOTTO; added to the plates; and incubated at 37°C for 45 min. The plates were washed 5 times with wash buffer (PBS–0.01% Tween 20), guinea pig anti-RV hyperimmune serum (provided by H. B. Greenberg) diluted 1:4,000 in 2.5% BLOTTO was added, and plates were incubated as described above for the previous step. After 5 washes, biotinylated anti-guinea pig serum (Vector Labs, Burlingame, CA, USA) diluted 1:2,000 in 2.5% BLOTTO was added, and the mixture was incubated at 37°C for 45 min. Peroxidase-labeled streptavidin (SeraCare, Milford, MA, USA) diluted 1:1,000 in 2.5% BLOTTO was added after 5 washes and incubated at 37°C for 30 min. Finally, a 1:1 tetramethylbenzidine (TMB)-hydrogen peroxide solution (SeraCare, Milford, MA, USA) was used to develop the reaction, which was stopped by the addition of 2 M sulfuric acid. The absorbance was read at a 450-nm wavelength on an ELISA plate reader (Multiskan EK; Thermolab Systems) to determine the optical density (OD). To determine the concentration of RV antigen in the samples, a calibration curve was made with the intestinal lysate of EC-RV-infected mouse pups, and results were expressed as the $\log_{10}$ SD_{50} per milliliter.

For the detection of intestinal RV-IgA, vinyl U-bottom plates were coated and blocked as described above for the antigen detection ELISA and then incubated with RRV or mock supernatants (1:10 in 5% BLOTTO) at 37°C for 1 h. After 5 washes, stool samples prepared as described above were added, and the mixture was incubated for 2 h at 37°C. The plates were washed 5 times, peroxidase-labeled antibody to mouse IgA (SeraCare, Milford, MA, USA) diluted 1:500 in 2.5% BLOTTO was added, and the mixture was incubated for 1 h at 37°C. The plates were washed and developed as described above for the antigen ELISA. A stool sample was considered to be positive for RV-IgA if the OD value was above 0.1 and twice the signal from the corresponding mock-treated wells.

Measurement of TGF-β by an ELISA. Total (active plus latent activated with HCl) TGF-β1 was quantified by an ELISA with a Duoset kit, according to the manufacturer's instructions (R&D Systems) (detection limit of 31.3 pg/ml).

Statistical analysis. Nonparametric statistics were used throughout the study. Comparisons between groups were performed with Mann-Whitney or Wilcoxon tests using the GraphPad Prism 6 program (GraphPad Software, Inc., San Diego, CA). In most figures, data medians are represented unless otherwise mentioned. A P value of <0.05 was considered statistically significant.

A generalized estimation equations (GEE) model using exchangeable working correlation and a Huber/White/sandwich estimator of variance was used to explore differences between the three antibody treatments. The average risk adjusted by day for each treatment effect, known as the population-averaged effect, is reported (47, 48). P values and confidence intervals for multiple comparisons between treatments were calculated by a Bonferroni inequality method (49).

SUPPLEMENTAL MATERIAL

Supplemental material for this article may be found at https://doi.org/10.1128/JVI.00882-19.

SUPPLEMENTAL FILE 1, PDF file, 2.4 MB.

ACKNOWLEDGMENTS

This project was funded by Colciencias grant 120365842530 and grant 00007684 from the Vicerrectoría de Investigación, Pontificia Universidad Javeriana. L.M.R. was funded by the Joven Investigador program from Colciencias and was awarded a partial scholarship by the Fundación Bolivar Davivienda. J.M. was supported by Ph.D. student fellowships from Colciencias and the Pontificia Universidad Javeriana (Convocatoria 727 Doctorados Nacionales). The NIH Tetramer Core Facility (which provided the tetramers for the study) is supported by contract HHSN272201300006C from the National Institute of Allergy and Infectious Diseases, a component of the National Institutes of Health of the Department of Health and Human Services.

We thank the personnel of UBC and especially Manuel Góngora and María Lucía Correal for help with the animal experiments and Camilo Vásquez for help with some of the flow cytometry experiments.

M.A.F., J.Á., and L.-S.R. contributed conception and design of the study and supervision of experiments. L.M.R. administered the virus and inhibitor to mice and performed surface and tetramer staining and ELISAs for RV antigen and IgA measurement. J.Á.G. was responsible for TGF-β ELISAs. J.M. helped with the intracellular cytokine assay. M.A.R. performed the statistical analysis. All authors analyzed the data and revised the manuscript.

We disclose no potential conflicts of interest.

Downloaded from http://jvi.asm.org/ on May 8, 2020 by guest

REFERENCES

1. Kelly A, Houston SA, Sherwood E, Casulli J, Travis MA. 2017. Regulation of innate and adaptive immunity by TGFbeta. Adv Immunol 134:137–233. https://doi.org/10.1016/bs.ai.2017.01.001.
2. Franco MA. 2016. Papel del TGF-β en la inmunidad contra los rotavirus. Rev Acad Colomb Cienc Ex Fis Nat 40:18–26. https://doi.org/10.18257/raccefyn.300.
3. Maizels RM, Smits HH, McSorley HJ. 2018. Modulation of host immunity by helminths: the expanding repertoire of parasite effector molecules. Immunity 49:801–818. https://doi.org/10.1016/j.immuni.2018.10.016.
4. Garidou L, Heydari S, Gossa S, McGavern DB. 2012. Therapeutic blockade of transforming growth factor beta fails to promote clearance of a persistent viral infection. J Virol 86:7060–7071. https://doi.org/10.1128/JVI.00164-12.
5. Boettler T, Cheng Y, Ehrhardt K, von Herrath M. 2012. TGF-beta blockade does not improve control of an established persistent viral infection. Viral Immunol 25:232–238. https://doi.org/10.1089/vim.2011.0079.
6. Woods PS, Tazi MF, Chesarino NM, Amer AO, Davis IC. 2015. TGF-beta-induced IL-6 prevents development of acute lung injury in influenza A virus-infected F508del CFTR-heterozygous mice. Am J Physiol Lung Cell Mol Physiol 308:L1136–L1144. https://doi.org/10.1152/ajplung.00078.2015.
7. Carlson CM, Turpin EA, Moser LA, O'Brien KB, Cline TD, Jones JC, Tumpey TM, Katz JM, Kelley LA, Gauldie J, Schultz-Cherry S. 2010. Transforming growth factor-beta: activation by neuraminidase and role in highly pathogenic H5N1 influenza pathogenesis. PLoS Pathog 6:e1001136. https://doi.org/10.1371/journal.ppat.1001136.
8. Denney L, Branchett W, Gregory LG, Oliver RA, Lloyd CM. 2018. Epithelial-derived TGF-beta1 acts as a pro-viral factor in the lung during influenza A infection. Mucosal Immunol 11:523–535. https://doi.org/10.1038/mi.2017.77.
9. Meliopoulos VA, Van de Velde LA, Van de Velde NC, Karlsson EA, Neale G, Vogel P, Guy C, Sharma S, Duan S, Surman SL, Jones BG, Johnson MD, Bosio C, Jolly L, Jenkins RG, Hurwitz JL, Rosch JW, Sheppard D, Thomas PG, Murray PJ, Schultz-Cherry S. 2016. An epithelial integrin regulates the amplitude of protective lung interferon responses against multiple respiratory pathogens. PLoS Pathog 12:e1005804. https://doi.org/10.1371/journal.ppat.1005804.
10. Rezende RM, Weiner HL. 2018. Cellular components and mechanisms of oral tolerance induction. Crit Rev Immunol 38:207–231. https://doi.org/10.1615/CritRevImmunol.2018026181.
11. Gabriely G, da Cunha AP, Rezende RM, Kenyon B, Madi A, Vandeventer T, Skillin N, Rubino S, Garo L, Mazzola MA, Kolypetri P, Lanser AJ, Moreira T, Faria AMC, Lassmann H, Kuchroo V, Murugaiyan G, Weiner HL. 2017. Targeting latency-associated peptide promotes antitumor immunity. Sci Immunol 2:eaaj1738. https://doi.org/10.1126/sciimmunol.aaj1738.
12. da Cunha AP, Wu HY, Rezende RM, Vandeventer T, Weiner HL. 2015. In vivo anti-LAP mAb enhances IL-17/IFN-gamma responses and abrogates anti-CD3-induced oral tolerance. Int Immunol 27:73–82. https://doi.org/10.1093/intimm/dxu083.
13. Rezende RM, Oliveira RP, Medeiros SR, Gomes-Santos AC, Alves AC, Loli FG, Guimaraes MA, Amaral SS, da Cunha AP, Weiner HL, Azevedo V, Miyoshi A, Faria AM. 2013. Hsp65-producing Lactococcus lactis prevents experimental autoimmune encephalomyelitis in mice by inducing CD4+LAP+ regulatory T cells. J Autoimmun 40:45–57. https://doi.org/10.1016/j.jaut.2012.07.012.
14. Moreira TG, Horta LS, Gomes-Santos AC, Oliveira RP, Queiroz N, Mangani D, Daniel B, Vieira AT, Liu S, Rodrigues AM, Gomes DA, Gabriely G, Ferreira E, Weiner HL, Rezende RM, Nagy L, Faria AMC. 2019. CLA-supplemented diet accelerates experimental colorectal cancer by inducing TGF-beta-producing macrophages and T cells. Mucosal Immunol 12:188–199. https://doi.org/10.1038/s41385-018-0090-8.
15. Butera A, Sanchez M, Pronio A, Amendola A, De Nitto D, Di Carlo N, Lande R, Frasca L, Borrini F, Pica R, Boirivant M. 2018. CD3+CD4+LAP+Foxp3− regulatory cells of the colonic lamina propria limit disease extension in ulcerative colitis. Front Immunol 9:2511. https://doi.org/10.3389/fimmu.2018.02511.
16. GBD 2016 Diarrhoeal Disease Collaborators. 2018. Estimates of the global, regional, and national morbidity, mortality, and aetiologies of diarrhoea in 195 countries: a systematic analysis for the Global Burden of Disease Study 2016. Lancet Infect Dis 18:1211–1228. https://doi.org/10.1016/S1473-3099(18)30362-1.
17. Herrera D, Parra M, Franco MA, Angel J. 2016. Human acquired immunity to rotavirus disease and correlates of protection, p 265–278. *In* Svensson L, Desselberger U, Greenberg HB, Estes MK (ed), Viral gastroenteritis. Elsevier, San Diego, CA.
18. Clarke E, Desselberger U. 2015. Correlates of protection against human rotavirus disease and the factors influencing protection in low-income settings. Mucosal Immunol 8:1–17. https://doi.org/10.1038/mi.2014.114.
19. Mesa MC, Gutiérrez L, Duarte-Rey C, Angel J, Franco MA. 2010. A TGF-β mediated regulatory mechanism modulates the T cell immune response to rotavirus in adults but not in children. Virology 399:77–86. https://doi.org/10.1016/j.virol.2009.12.016.
20. Parra M, Herrera D, Jácome MF, Mesa MC, Rodríguez LS, Guzmán C, Angel J, Franco MA. 2014. Circulating rotavirus-specific T cells have a poor functional profile. Virology 468–470:340–350. https://doi.org/10.1016/j.virol.2014.08.020.
21. Rodríguez L-S, Barreto A, Franco MA, Angel J. 2009. Immunomodulators released during rotavirus infection of polarized Caco-2 cells. Viral Immunol 22:163–172. https://doi.org/10.1089/vim.2008.0110.
22. Rodriguez LS, Narvaez CF, Rojas OL, Franco MA, Angel J. 2012. Human myeloid dendritic cells treated with supernatants of rotavirus infected Caco-2 cells induce a poor Th1 response. Cell Immunol 272:154–161. https://doi.org/10.1016/j.cellimm.2011.10.017.
23. Franco MA, Greenberg HB. 1999. Immunity to rotavirus infection in mice. J Infect Dis 179(Suppl 3):S466–S469. https://doi.org/10.1086/314805.
24. Franco MA, Greenberg HB. 1995. Role of B cells and cytotoxic T lymphocytes in clearance of and immunity to rotavirus infection in mice. J Virol 69:7800–7806.
25. Jaimes MC, Feng N, Greenberg HB. 2005. Characterization of homologous and heterologous rotavirus-specific T-cell responses in infant and adult mice. J Virol 79:4568–4579. https://doi.org/10.1128/JVI.79.8.4568-4579.2005.
26. VanCott JL, Prada AE, McNeal MM, Stone SC, Basu M, Huffer B, Jr, Smiley KL, Shao M, Bean JA, Clements JD, Choi AH, Ward RL. 2006. Mice develop effective but delayed protective immune responses when immunized as neonates either intranasally with nonliving VP6/LT(R192G) or orally with live rhesus rotavirus vaccine candidates. J Virol 80:4949–4961. https://doi.org/10.1128/JVI.80.10.4949-4961.2006.
27. Burns JW, Krishnaney AA, Vo PT, Rouse RV, Anderson LJ, Greenberg HB. 1995. Analyses of homologous rotavirus infection in the mouse model. Virology 207:143–153. https://doi.org/10.1006/viro.1995.1060.
28. Feng N, Burns JW, Bracy L, Greenberg HB. 1994. Comparison of mucosal and systemic humoral immune responses and subsequent protection in mice orally inoculated with a homologous or a heterologous rotavirus. J Virol 68:7766–7773.
29. Masopust D, Vezys V, Usherwood EJ, Cauley LS, Olson S, Marzo AL, Ward RL, Woodland DL, Lefrancois L. 2004. Activated primary and memory CD8 T cells migrate to nonlymphoid tissues regardless of site of activation or tissue of origin. J Immunol 172:4875–4882. https://doi.org/10.4049/jimmunol.172.8.4875.
30. Obar JJ, Jellison ER, Sheridan BS, Blair DA, Pham QM, Zickovich JM, Lefrancois L. 2011. Pathogen-induced inflammatory environment controls effector and memory CD8+ T cell differentiation. J Immunol 187:4967–4978. https://doi.org/10.4049/jimmunol.1102335.
31. Obar JJ, Sheridan BS. 2015. Tracking cytotoxic potential in vivo. Cell Mol Immunol 12:505–507. https://doi.org/10.1038/cmi.2014.69.
32. Herndler-Brandstetter D, Ishigame H, Shinnakasu R, Plajer V, Stecher C, Zhao J, Lietzenmayer M, Kroehling L, Takumi A, Kometani K, Inoue T, Kluger Y, Kaech SM, Kurosaki T, Okada T, Flavell RA. 2018. KLRG1(+) effector CD8(+) T cells lose KLRG1, differentiate into all memory T cell lineages, and convey enhanced protective immunity. Immunity 48:716.e8–729.e8. https://doi.org/10.1016/j.immuni.2018.03.015.
33. Beyersdorf N, Ding X, Tietze JK, Hanke T. 2007. Characterization of mouse CD4 T cell subsets defined by expression of KLRG1. Eur J Immunol 37:3445–3454. https://doi.org/10.1002/eji.200737126.
34. Cheng G, Yuan X, Tsai MS, Podack ER, Yu A, Malek TR. 2012. IL-2 receptor signaling is essential for the development of Klrg1+ terminally differentiated T regulatory cells. J Immunol 189:1780–1791. https://doi.org/10.4049/jimmunol.1103768.
35. Chanda S, Nandi S, Chawla-Sarkar M. 2016. Rotavirus-induced miR-142-5p elicits proviral milieu by targeting non-canonical transforming growth factor beta signalling and apoptosis in cells. Cell Microbiol 18:733–747. https://doi.org/10.1111/cmi.12544.

Downloaded from http://jvi.asm.org/ on May 8, 2020 by guest

36. Parra M, Herrera D, Calvo-Calle JM, Stern LJ, Parra-López CA, Butcher E, Franco M, Angel J. 2014. Circulating human rotavirus specific CD4 T cells identified with a class II tetramer express the intestinal homing receptors $\alpha 4\beta 7$ and CCR9. Virology 452–453:191–201. https://doi.org/10.1016/j.virol.2014.01.014.
37. Plumlee CR, Obar JJ, Colpitts SL, Jellison ER, Haining WN, Lefrancois L, Khanna KM. 2015. Early effector CD8 T cells display plasticity in populating the short-lived effector and memory-precursor pools following bacterial or viral infection. Sci Rep 5:12264. https://doi.org/10.1038/srep12264.
38. Wen K, Li G, Yang X, Bui T, Bai M, Liu F, Kocher J, Yuan L. 2012. CD4+ CD25− FoxP3+ regulatory cells are the predominant responding regulatory T cells after human rotavirus infection or vaccination in gnotobiotic pigs. Immunology 137:160–171. https://doi.org/10.1111/j.1365-2567.2012.03617.x.
39. Kim B, Feng N, Narvaez CF, He XS, Eo SK, Lim CW, Greenberg HB. 2008. The influence of CD4+ CD25+ Foxp3+ regulatory T cells on the immune response to rotavirus infection. Vaccine 26:5601–5611. https://doi.org/10.1016/j.vaccine.2008.07.099.
40. Miller AD, Blutt SE, Conner ME. 2014. FoxP3+ regulatory T cells are not important for rotavirus clearance or the early antibody response to rotavirus. Microbes Infect 16:67–72. https://doi.org/10.1016/j.micinf.2013.09.004.
41. Franco MA, Tin C, Greenberg HB. 1997. CD8+ T cells can mediate almost complete short-term and partial long-term immunity to rotavirus in mice. J Virol 71:4165–4170.
42. Mesa MC, Rodríguez L-S, Franco MA, Angel J. 2007. Interaction of rotavirus with human peripheral blood mononuclear cells: plasmacytoid dendritic cells play a role in stimulating memory rotavirus specific T cells in vitro. Virology 366:174–184. https://doi.org/10.1016/j.virol.2007.04.007.
43. Franco MA, Tin C, Rott LS, VanCott JL, McGhee JR, Greenberg HB. 1997. Evidence for CD8$^+$ T-cell immunity to murine rotavirus in the absence of perforin, fas, and gamma interferon. J Virol 71:479–486.
44. National Research Council. 2011. Guide for the care and use of laboratory animals, 8th ed. National Academies Press, Washington, DC.
45. Fahlen L, Read S, Gorelik L, Hurst SD, Coffman RL, Flavell RA, Powrie F. 2005. T cells that cannot respond to TGF-beta escape control by CD4(+)CD25(+) regulatory T cells. J Exp Med 201:737–746. https://doi.org/10.1084/jem.20040685.
46. Grainger JR, Smith KA, Hewitson JP, McSorley HJ, Harcus Y, Filbey KJ, Finney CA, Greenwood EJ, Knox DP, Wilson MS, Belkaid Y, Rudensky AY, Maizels RM. 2010. Helminth secretions induce de novo T cell Foxp3 expression and regulatory function through the TGF-beta pathway. J Exp Med 207:2331–2341. https://doi.org/10.1084/jem.20101074.
47. Zeger SL, Liang KY, Albert PS. 1988. Models for longitudinal data: a generalized estimating equation approach. Biometrics 44:1049–1060. https://doi.org/10.2307/2531734.
48. Ziegler A, Vens M. 2014. Generalized estimating equations, p 1337–1376. *In* Ahrens W, Pigeot I (ed), Handbook of epidemiology. Springer, New York, NY.
49. Hsu JC. 2016. Multiple comparisons: theory and methods, 1st ed. CRC Press, Boca Raton, FL.

Downloaded from http://jvi.asm.org/ on May 8, 2020 by guest